

Very hard states in neutron star low-mass X-ray binaries

A. S. Parikh,¹★ R. Wijnands,¹ N. Degenaar,¹ D. Altamirano,² A. Patruno,³
N. V. Gusinskaia¹ and J. W. T. Hessels^{1,4}

¹*Anton Pannekoek Institute for Astronomy, University of Amsterdam, Postbus 94249, NL-1090 GE Amsterdam, the Netherlands*

²*Department of Physics and Astronomy, Southampton University, Southampton SO17 1BJ, UK*

³*Leiden Observatory, Leiden University, Postbus 9513, NL-2300 RA Leiden, the Netherlands*

⁴*ASTRON, the Netherlands Institute for Radio Astronomy, Postbus 2, NL-7990 AA Dwingeloo, the Netherlands*

Accepted 2017 March 23. Received 2017 March 22; in original form 2017 February 7

ABSTRACT

We report on unusually very hard spectral states in three confirmed neutron-star low-mass X-ray binaries (1RXS J180408.9–342058, EXO 1745–248 and IGR J18245–2452) at a luminosity between $\sim 10^{36}$ and 10^{37} erg s^{−1}. When fitting the *Swift* X-ray spectra (0.5–10 keV) in those states with an absorbed power-law model, we found photon indices of $\Gamma \sim 1$, significantly lower than the $\Gamma = 1.5$ –2.0 typically seen when such systems are in their so called hard state. For individual sources, very hard spectra were already previously identified, but here we show for the first time that likely our sources were in a distinct spectral state (i.e. different from the hard state) when they exhibited such very hard spectra. It is unclear how such very hard spectra can be formed; if the emission mechanism is similar to that operating in their hard states (i.e. up-scattering of soft photons due to hot electrons), then the electrons should have higher temperatures or a higher optical depth in the very hard state compared to those observed in the hard state. By using our obtained Γ as a tracer for the spectral evolution with luminosity, we have compared our results with those obtained by Wijnands et al. Our sample of sources follows the same track as the other neutron star systems in Wijnands et al., confirming their general results. However, we do not find that the accreting millisecond pulsars are systematically harder than the non-pulsating systems.

Key words: accretion, accretion discs – binaries: close – stars: neutron – X-rays: binaries.

1 INTRODUCTION

Low-mass X-ray binaries (LMXBs) have a compact object, a neutron star (NS) or a black hole (BH), as the primary object, and a low-mass donor star ($\lesssim 1 M_{\odot}$). The donor star facilitates accretion on to the compact object by overflowing its Roche lobe. Transient LMXBs undergo outbursts lasting weeks to years with outburst X-ray luminosities of $L_X \sim 10^{35}$ – 10^{38} erg s^{−1}, amidst periods of quiescence (with $L_X \lesssim 10^{34}$ erg s^{−1}) that last months to decades.

Many LMXBs are observed to have spectra that become softer with decreasing luminosity below $L_X \lesssim 10^{36}$ erg s^{−1} (e.g. Armas Padilla et al. 2011; Reynolds et al. 2014). This can be studied by fitting a phenomenological power-law model to the spectra and using the photon index Γ to trace the spectral evolution. The associated Γ 's display an anti-correlation with L_X in the 0.5–10 keV band. Wijnands et al. (2015) assembled a sample of sources for which they plotted Γ against L_X . NSs soften with decreasing luminosities below $L_X \lesssim 10^{36}$ erg s^{−1} (with a typical Γ of ~ 1.8) down to $L_X \sim 10^{34}$ erg s^{−1} ($\Gamma \sim 3$). In contrast, BHs are observed to soften only from $\Gamma \sim 1.5$ at around $L_X \sim 10^{34}$ erg s^{−1} increasing to about

$\Gamma \sim 2$ at $L_X \sim 10^{33}$ erg s^{−1} without further softening at lower L_X . Because of this different behaviour, BHs and NSs describe two separate tracks in the Γ versus L_X diagram, although this needs confirmation by studying more sources.

It is typically observed (and therefore commonly assumed) that when the 0.5–10 keV spectra of NS LMXBs are fitted with a power-law model, the photon index can only be as low as $\Gamma \sim 1.5$ –2.0 (e.g. Lewis et al. 2010; Degenaar et al. 2012; Bahramian et al. 2013; Wijnands et al. 2015). However, in our recent paper (Parikh et al. 2017), we studied the transient LMXB 1RXS J180408.9–342058. During this analysis, we found that at the beginning of its 2015 outburst, the source displayed very hard spectra with photon indices of $\Gamma \sim 1$ (in the energy range 0.5–10 keV; in the rest of the paper we will always assume this energy range for the determination of Γ). This is much harder than expected. Here, we study several sources with similar very hard spectra to confirm the existence of such a very hard state in multiple NS systems.

2 SOURCE SELECTION AND DATA ANALYSIS

The very hard spectra of 1RXS J180408.9–342058 prompted us to search the literature for more sources that may also display such

* E-mail: a.s.parikh@uva.nl

spectral hardness. The recent paper by Tetarenko et al. (2016) reported that EXO 1745–248 showed unusual very hard spectra during the beginning of its 2015 outburst. In addition, we also found that IGR J18245–2452 and SAX J1748.9–2021 were reported to be similarly very hard (Ferrigno et al. 2014; Linares et al. 2014; Bozzo, Kuulkers & Ferrigno 2015). Finally, Del Santo et al. (2014) proposed a tidal disruption event by a planet on to a white dwarf for IGR J17361–4441, but Wijnands et al. (2015) put forth an LMXB nature. Since an NS accretor is not firmly ruled out, we included it in our sample.

Using these, we noted that two of the systems (IGR J18245–2452 and SAX J1748.9–2021) are accreting millisecond X-ray pulsars (AMXPs; Altamirano et al. 2008; Papitto et al. 2013). It was noted by Wijnands et al. (2015, although based on limited amount of data) that AMXPs might, at similar L_x , show slightly harder spectra than non-pulsating NS systems. We considered the possibility that the pulsating nature of those sources (thus the presence of a dynamically important magnetic field) might be related to the very hard spectra of the two AMXPs in our sample. To test this hypothesis, we also included the canonical AMXP SAX J1808.4–3658 in our study. This AMXP was chosen as it has been extensively monitored by *Swift*/XRT (the instrument we use in our study; see below; Patruno et al. 2016). The other five sources have also been well monitored using this instrument. In case multiple outbursts were observed for a given source, only the well-sampled outbursts were considered (i.e. the evolution of the outburst was well monitored; based on this criterion we excluded the 2011 outburst of EXO 1745–248, the 2011 outburst of SAX J1808.4–3658 and the 2012 outburst of 1RXS J180408.9–342058). We only include well-sampled outbursts as we wish to track the spectral evolution of the source to ensure that our fit results are not just a statistical fluctuation, which could be the case if we consider single sparse pointings.

We followed the spectral evolution of our six sources by fitting a simple absorbed power-law model to all spectra. This allowed us to determine if those sources indeed exhibited very hard spectra but it also allowed us to carry out a follow-up study of Wijnands et al. (2015) to determine if their conclusions still hold when more sources are studied. The Wijnands et al. (2015) data we compare to in this paper corresponds to their fig. 1; we use all the BH data and the NS data that only corresponds to non-pulsating systems with low N_H .

The data were downloaded from the HEASARC archive and were analysed using HEASOFT (version 6.17). To process the raw data we used XRTPIPELINE. Circular extraction regions were used to extract the source spectra in XSELECT. Depending on the brightness of a given source, we used extraction regions with a radius varying between 25 and 100 arcsec. We used annular regions to account for the background in both window timing (WT) and photon counting (PC) modes (varying between 125 and 300 arcsec for the inner radius and 200 and 475 arcsec for the outer radius). For PC mode observations of sources located in globular clusters (see Table 1), the source flux is only a factor of a few above the background caused by other low-luminosity sources in the cluster and hence the normal background subtraction method cannot be used. For these observations, we extracted spectra from observations when the source was quiescent, using a similar region as when it was active, to serve as the background correction. The backscale keyword was set to correctly scale for different source and background regions.¹ The ancillary response files were created using XRTMKARF. The relevant response

Table 1. The Galactic and best-fitting N_H , and distance used for each source.^a

Source	N_H (10^{22} cm $^{-2}$)		Distance (kpc)
	Galactic	Best fit	
1RXS J180408.9–342058	0.20	0.41	5.8
EXO 1745–248	1.10	2.42	5.5
IGR J18245–2452	0.26	0.51	5.5
SAX J1748.9–2021	0.57	1.41	8.5
IGR J17361–4441	0.25	0.26	13.2
SAX J1808.4–3658	0.14	– ^b	3.5

Notes. ^aThe sources located in globular clusters are EXO 1745–248 (Terzan 5), IGR J18245–2452 (M28), SAX J1748.9–2021 (NGC 6440) and IGR J17361–4441 (NGC 6388). The respective references for the Galactic N_H values of the cluster sources are Degenaar & Wijnands (2012), Harris (1996); $E(B - V) = 0.4$, Pintore et al. (2016) and Bellini et al. (2013); $E(B - V) = 0.37$. The source distances are obtained from the following references (given in order): Chenevez et al. (2012), Ortolani et al. (2007), Harris (1996, using the updated version of 2010), Ortolani, Barbuy & Bica (1994), Dalessandro et al. (2008) and Galloway & Cumming (2006).

^bNo best-fitting N_H was calculated for SAX J1808.4–3658 (see Appendix A in the Supporting Information available online).

matrix files for each observation were used. Each spectrum was grouped using *grppha* – at least 10 photons per bin for the WT mode and at least 5 photons per bin for the PC mode. All type-I thermonuclear bursts were removed and all the relevant observations (i.e. when the source was relatively bright) were corrected for pile-up.²

The spectra from the various observations were fitted in XSPEC (version 12.9) with an absorbed POWERLAW model using W-statistics (background subtracted Cash statistics; Wachter, Leach & Kellogg 1979) because of the low number of photons per bin. The TBABS component was used to model the hydrogen column density N_H using VERN cross-sections and WILM abundances (Verner et al. 1996; Wilms, Allen & McCray 2000). The value of N_H used is discussed further in Section 3. Due to the low energy spectral residuals in the WT mode, the WT mode data were fit over the 0.7–10 keV range.³ The PC data were fit over the 0.5–10 keV range. All the fluxes reported are the unabsorbed fluxes, determined using the convolution model *cf1ux* in the 0.5–10 keV range. Luminosities are also given for the 0.5–10 keV range, and errors correspond to the 90 per cent confidence range.

3 RESULTS

The obtained values of the various parameters resulting from our spectral fits are systematically affected by our assumptions and data reduction. Some of these effects, such as those introduced by distance, pile-up and fitting a simple model to a more complex spectral shape, have been discussed by Wijnands et al. (2015). The distances used for the various sources are shown in Table 1. Wijnands et al. (2015) also briefly discussed the effect of fitting a simple model to high-quality data and the effect of the N_H value assumed. Here, we discuss the effect of the assumed N_H value in more detail, in relation to our analysis method. Abundances and cross-sections may have a systematic effect on Γ . Using different abundances changes the absolute value slightly (see appendix A of

¹ <http://www.swift.ac.uk/analysis/xrt/backscal.php>

² <http://www.swift.ac.uk/analysis/xrt/pileup.php>

³ http://www.swift.ac.uk/analysis/xrt/digest_cal.php

Plotkin et al. 2016); however, our conclusions do not change when using different cross-sections and abundances.

From our analysis, we found that if the N_H was left free in the spectral fits, the N_H traced a large range of values (for a given source), especially if the source exhibited different spectral states (e.g. Fig. A.1 in the Supporting Information available online). This change in the N_H directly affects the Γ of the fit as the two components are correlated – the Γ value increases if the N_H increases (see e.g. Plotkin, Gallo & Jonker 2013). Since we want to use Γ as a tracer for spectral hardness, this degeneracy is undesirable. To prevent this issue, we fit the spectra by fixing the N_H to a particular value, although it was not directly clear to what value we should fix it. In other spectral studies of our sources, the N_H values used were either the Galactic (line-of-sight extinction) values or the values obtained when N_H was left free in spectral fits to high-quality data. In the end, we analysed our data considering all three approaches: (1) leaving the N_H free, (2) fixing it to the Galactic N_H and (3) fixing it to the best-fitting N_H .

For the four sources located in globular clusters (see Table 1), the Galactic N_H was determined using the known reddening $E(B - V)$, or N_H values previously determined from high-quality data were used. If the N_H was calculated from the $E(B - V)$ values, the relationship given by Güver & Özel (2009; see also Predehl & Schmitt 1995) was used for the conversion. For the remaining two sources (1RXS J180408.9–342058 and SAX J1808.4–3658), the Galactic N_H was determined using Dickey & Lockman (1990). The Galactic values of N_H are shown in Table 1.

We determine the best-fitting N_H ourselves. This is done by initially leaving the N_H free and fitting the various observations with an absorbed power-law model getting various N_H values. Then, we fit a constant to the obtained N_H values to get the best-fitting N_H . If a source is known to show a hard to soft state transition, only the data from the hard state is used to determine the constant since it is known that in the hard state a power-law model can typically describe the spectra reasonably adequately (i.e. when the data quality is low); whereas in the soft state, the spectra are more complex. Therefore, the N_H obtained in this way will best resemble the true N_H . The evolution of the free N_H with time as well as the constant fit (to the relevant observations) is shown in Appendix A (see the Supporting Information available online), where we describe how the best-fitting N_H was determined in more detail. All the calculated best-fitting N_H values are shown in Table 1. SAX J1808.4–3658 (see Appendix A in the Supporting Information available online) showed a different N_H evolution for each of the three outbursts we consider. It also showed N_H evolution within each outburst. Thus, calculating the best-fitting N_H for this source was not straightforward. Therefore, we have not determined a best-fitting N_H for SAX J1808.4–3658. Our values for the other sources are consistent with those reported in the literature (Degenaar & Wijnands 2012; Papitto et al. 2013; Linares et al. 2014; Del Santo et al. 2014; Bozzo et al. 2015; Degenaar et al. 2016; Ludlam et al. 2016; Pintore et al. 2016; Tetarenko et al. 2016).

To understand which N_H method to use to compare our targets with the Wijnands et al. (2015) results, we studied the literature references for the data they used to determine how the original papers obtained the spectral fits. We concluded that in (nearly) all results the N_H was obtained by using it as a free parameter in the fit.

3.1 Photon index versus luminosity

To maintain consistency with Wijnands et al. (2015), we disregarded all fits that have an error >0.5 on Γ . In the case where we left the

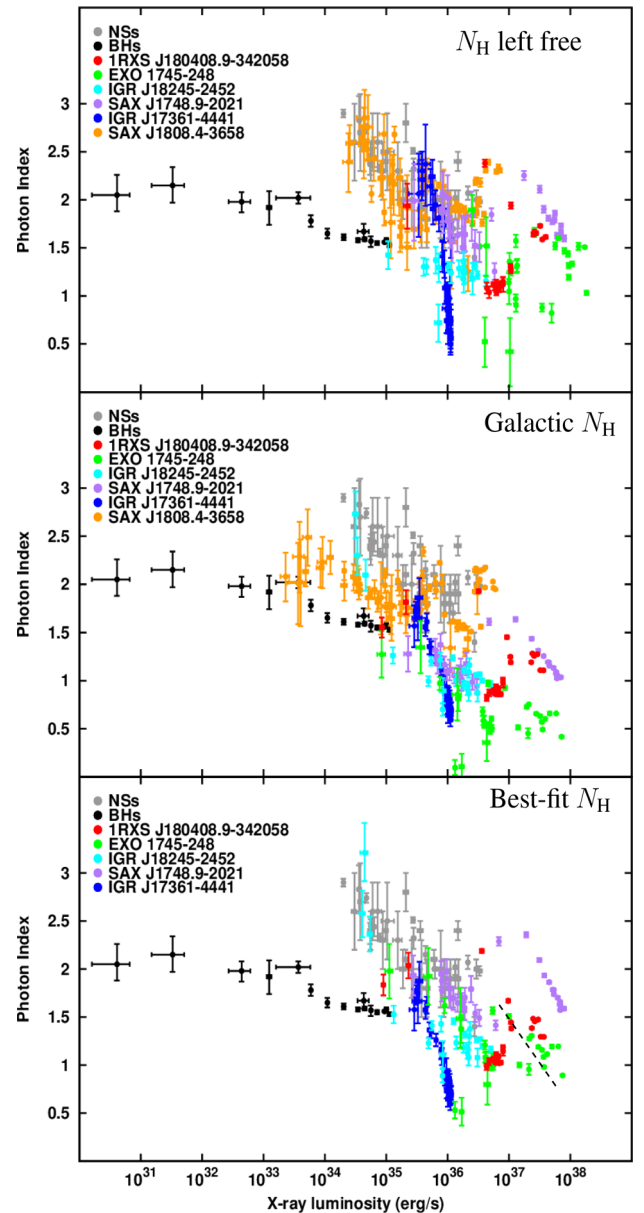


Figure 1. The photon index versus luminosity (0.5–10 keV) for various NS (shown in grey) and BH (shown in black) X-ray binaries taken from fig. 1 of Wijnands et al. (2015) along with our targets. The top panel indicates data when N_H is a free parameter in the fits, the central panel when N_H is fixed to the Galactic value and the bottom panel when the N_H is fixed to the best-fitting value. No best-fitting N_H value for SAX J1808.4–3658 was calculated (see Appendix A in the Supporting Information available online) and therefore the data are not plotted in the lowest panel. The dashed black line in the lowest panel indicates the hard to soft state transition for 1RXS J180408.9–342058 and EXO 1745–248. [A colour version of this figure is available in the online version.]

N_H free, the errors were systematically larger than in the other two cases, resulting in ~ 10 per cent fewer points (see Fig. 1). The Γ versus L_X values of our six sources, using different assumptions for the N_H value, are plotted in Fig. 1 along with the results from Wijnands et al. (2015). The individual Γ versus L_X plots for each source as well as the tabulated values are presented in Fig. C.1 and Appendix D (see the Supporting Information available online). We compared our results with previously published results of our

sources and we found that they are consistent with those results when similar spectral states were analysed (Ferrigno et al. 2011; Del Santo et al. 2014; Linares et al. 2014; Bozzo et al. 2015; Wijnands et al. 2015; Tetarenko et al. 2016).

The data in the top panel of Fig. 1, when N_{H} is left free, indicate the unusually very hard spectra (with $\Gamma \sim 0.5\text{--}1.3$ over the luminosity range $L_{\text{X}} \sim 10^{36}\text{--}10^{37}$ erg s $^{-1}$) of our five confirmed NS LMXBs, although SAX J1748.9–2021 and SAX J1808.4–3658 show only a few data points with very hard spectra and by themselves would not necessarily prove the existence of very hard spectra. However, the combined sample clearly shows the presence of a very hard state. The unclassified source IGR J17361–4441 also shows very hard photon indices of $\Gamma \sim 0.5\text{--}1$ but at slightly lower luminosity $L_{\text{X}} \sim 10^{36}$ erg s $^{-1}$. Appendix B (see the Supporting Information available online) shows the evolution of Γ with time, when N_{H} is left free. Besides the existence of apparently very hard spectra in our targets, Fig. 1, top panel, also shows that below $L_{\text{X}} \lesssim 10^{36}$ erg s $^{-1}$, most of our targets behave in a manner that is in agreement with the results of Wijnands et al. (2015), although IGR J18245–2452 appears to remain very hard between $L_{\text{X}} \sim 10^{35}$ and 10^{36} erg s $^{-1}$ and for 1RXS J180408.9–342058 there is no data available in this range.

The central panel and bottom panel of Fig. 1 show the data assuming the Galactic N_{H} and the best-fitting N_{H} , respectively. In the middle panel, the Γ for all points compared to the free N_{H} (top panel, Fig. 1) decreases significantly. Since the Galactic N_{H} are consistently lower than the free N_{H} (see Table 1) it causes the observed decrease of Γ . Similarly, a softening of Γ is observed when the best-fitting N_{H} is used (lowest panel Fig. 1) compared to the Galactic N_{H} as the best-fitting N_{H} tends to be higher.

When assuming the Galactic N_{H} value in our fits, SAX J1808.4–3658 does not fall on the standard NS track but it forms a separate track at significantly lower Γ s. However, since the data points used by Wijnands et al. (2015) were mostly obtained using a different N_{H} criteria (see Section 3), we cannot directly compare SAX J1808.4–3658 and any of the other sources with this track. Therefore, we will no longer discuss the Galactic N_{H} results further when comparing our sample to the Wijnands et al. (2015) results.

From Fig. 1, lower panel, it can be seen that, when using the best-fitting N_{H} , only four of our six sources display very hard spectra with $\Gamma \sim 1$. Those sources are 1RXS J180408.9–342058, EXO 1745–248, IGR J18245–2452 and IGR J17361–4441. No best-fitting N_{H} was calculated for SAX J1808.4–3658 (see Appendix A in the Supporting Information available online), and therefore it has not been plotted. From the different panels in Fig. 1, it can be seen that for the AMXP SAX J1748.9–2021 the inferred spectral hardness strongly depends on the N_{H} value used. When using the Galactic N_{H} in our spectral fits, the source appears to show a very hard spectra ($\Gamma \sim 1$; Fig. 1, middle panel). This is consistent with the *Swift*/XRT results published by Bozzo et al. (2015) who assumed this N_{H} . However, when leaving the N_{H} free (top panel) or fixing it to the best-fitting N_{H} , the spectra appear softer and this source is then fully consistent with the standard NS track.

The dashed black line in the lowest panel of Fig. 1 indicates the hard to soft state transition for 1RXS J180408.9–342058 and EXO 1745–248. The soft state shows the presence of very hard spectra as well; however this is an artefact of using too low N_{H} compared to when N_{H} is left free (as seen in Fig. A 1) and thus we get too low Γ s (compare bottom with top panel for EXO 1745–248). In addition, the soft, thermal component that becomes visible could have temperatures well above a few keV possibly resulting in very hard spectra if one fits with a power-law model in the 0.5–10 keV range (see Section 4).

4 DISCUSSION

We have studied the spectra (using an absorbed power-law model) of six seemingly very hard (candidate) NS LMXBs. The Γ values obtained from the spectral fits are strongly dependent on our assumptions about the N_{H} values. We find that four sources indeed show very hard spectra down to $\Gamma \sim 1$ (see Fig. 1) irrespective of the approach used to determine N_{H} . The cause of these very hard spectra is unknown. Hard X-rays are expected to be produced by Compton up-scattering of soft photons by hot electrons (e.g. that are present in a corona, an accretion column or a possible boundary layer). The unusual very low Γ may be a result of higher electron temperatures or higher optical depths of this Comptonizing medium than those present during the typically observed hard NS state. Our results suggest that we might have identified a new spectral state in NS LMXBs. This conclusion is strengthened by the different rapid X-ray variability properties we observed during this state compared to the hard state of those sources (see Wijnands et al., in preparation).

Measurements of the spectra above 10 keV would be useful to investigate the physical process behind such very hard spectra. 1RXS J180408.9–342058 is a promising candidate as it has good coverage over a large energy range in several different spectral states. The source has been studied by Ludlam et al. (2016, in the energy range 0.45–50 keV) when the source was in this very hard state and by Degenaar et al. (2016, for 0.7–35 keV) when it was in the soft state. Comparing the obtained spectra with each other could elucidate the physical mechanism behind the very hard state. However, to do this the spectra have to be reanalysed in a homogenous manner and we are currently performing such reanalysis. The results of this will be reported elsewhere. Here, we only wish to stress the existence of a very hard spectral state in NS LMXBs, which is important in studies that classify such systems based on spectral hardness alone and this new spectral state needs to be accounted for in models that aim to explain the accretion physics in such systems. In addition, more NS sources need to be studied to determine what fraction of NSs show this very hard state and to determine if some physical property is associated with the presence of such very hard spectra. Also the BH systems need to be studied to check if they can display similar very hard states. If such states are also present in BH systems it would indicate that the physical mechanism in the accretion flow that generates such very hard spectra is not (or only minorly) affected by the presence of an NS surface and/or magnetic field or a BH event horizon. The *Swift*/XRT data base contains many archival observations that can be used to extend this study for NSs and BHs.

We also compare our data to that reported by Wijnands et al. (2015). For luminosities below $L_{\text{X}} \lesssim 10^{36}$ erg s $^{-1}$, all sources but one (IGR J18245–2452) line up with the expected NS track when using similar N_{H} assumptions as used for the points in Wijnands et al. (2015, see section 3). Although IGR J18245–2452 does not follow the NS track at around $\sim 10^{36}$ erg s $^{-1}$, at the lowest luminosities (a few times 10^{34} erg s $^{-1}$), the source joins the track (Fig. 1, bottom; see also Wijnands et al. 2015; those points are absent in Fig. 1 top because the N_{H} was left free in that plot resulting in such large errors on Γ that those point fell outside our selection criteria). If more sources are added to the sample, the assumptions on the N_{H} should be the same as those used by us: i.e. the N_{H} should ideally be left free but if that is not possible because of the low statistical quality of the data then the N_{H} should be fixed to the value obtained from higher quality data of the same source.

The absolute value of Γ should not be taken at face value since we fit a phenomenological model. The fit parameter Γ can only be

used to study the broad evolution – hardening and softening of the spectra of a given source, and to compare different sources with one another. Another limitation is that we fit only the 0.5–10 keV energy range that might mask spectral evolution. In particular, in the soft state, blackbody-type components are often observed in the spectra and they can have high temperatures (up to several keV). Such spectra below 10 keV still appear as quite hard with relatively low Γ (when fitted with a power-law model). This can be clearly seen in Fig. 1 (bottom) where we draw the line between soft and hard state in 1RXS J180408.9–342058 and EXO 1745–248.

An added complication at the highest luminosities is that during broad-band studies using X-ray colours of NS LMXBs (i.e. using hardness–intensity diagrams) it has been found that some sources that accrete at a few tenths of the Eddington rate show the same colours (and hence the same spectral shape) in the soft state at different count rates [and thus different L_X ; this is referred to as secular motion; see Homan et al. 2010 (i.e. their Fig. 1) and Fridriksson, Homan & Remillard 2015 for discussion about this and further references]. Although most of these studies were done over a different energy range than the 0.5–10 keV range, it is plausible that a similar effect is visible in the 0.5–10 keV energy range. For example, this can be seen in SAX J1808.4–3658, although at lower luminosities than typically seen in those other studies. So we urge the reader to be cautious in how to interpret the data points of the sources at their highest L_X .

IGR J17361–4441 is an unusual transient that is not easily classified. Based on its luminosity evolution together with its odd spectra (and how it evolved in time), Del Santo et al. (2014) classified the source as a tidal disruption event of a planet sized body by a white dwarf. Its spectra were odd as they were very hard (with $\Gamma \sim 1$ and even lower; see also Fig. 1) and showed the presence of a soft component with very low temperatures (~ 0.08 keV) that did not change when the luminosity decreased at the end of the outburst. However, we have now found that three confirmed NS transients show similar very hard spectra (1RXS J180408.9–342058, EXO 1745–248 and IGR J18245–2452). The source remains enigmatic (it is the hardest source in our sample, the Γ versus L_X behaviour is very steep compared to the other systems, and it is unclear how to explain the constant soft component). However, at low L_X , the source joins the normal NS track for all values of N_H used. Combined with a power spectrum that looks similar to that of accreting NSs or BHs (see the appendix of Wijnands et al. 2015; but see Bozzo et al. 2014 for an interpretation of these results as a tidal disruption event), this suggests that an NS LMXB nature cannot be discarded for IGR J17361–4441.

In our analysis, we have studied three AMXPs: SAX J1748.9–2021 (an intermittent AMXP), IGR J18245–2452 (a transitional millisecond pulsar; a special subset of AMXPs; e.g. Archibald et al. 2009; Papitto et al. 2013) and SAX J1808.4–3658 (the ‘canonical’ AMXP). Linares et al. (2014) and Ferrigno et al. (2014) reported on the *Swift*/XRT and *XMM-Newton* spectra of IGR J18245–2452 and noted the hardness of the spectra in this source. They briefly discussed this in the context of the source being a transitional millisecond pulsar and that the NS magnetic field in this system might be related to its very hard spectra. Wijnands et al. (2015) tentatively proposed that AMXPs are systematically harder (in the L_X range of 10^{34} – 10^{36} erg s $^{-1}$) than non-pulsating NSs, although they highlighted that this hypothesis was only based on limited AMXP data and needed confirmation. In our study, we found that indeed IGR J18245–2452 is harder than the non-pulsating systems at $L_X \sim 10^{36}$ erg s $^{-1}$, although it joins the track at

lower L_X . We note that this source was one of the sources used by Wijnands et al. (2015) so it is not surprising that we reproduce their results. However, we found that SAX J1748.9–2021 does not show harder than average spectra if the N_H is left free or fixed to the best-fitted one (Fig. 1, top and bottom panels). However, this may be because it only pulsates intermittently and most of the time the source behaves like a non-pulsating NS (Altamirano et al. 2008; Patruno et al. 2009). SAX J1808.4–3658 also does not seem to display harder spectra (the caveats for the comparison with Wijnands et al. (2015) should be recalled). In addition, out of the four sources that exhibit very hard spectra – EXO 1745–248, IGR J17361–4441 and 1RXS J180408.9–342058 are non-pulsating sources (Wijnands et al. 2005; Bozzo et al. 2011). IGR J18245–2452 is an AMXP and shows pulsations (Papitto et al. 2013). This, combined with the fact that not all AMXPs are harder than non-pulsating systems, suggests that the hardness of the source spectra does not have a strict connection (if any at all) with the presence of a dynamically important magnetic field.

ACKNOWLEDGEMENTS

AP and RW are supported by a NWO Top Grant, awarded to RW. ND is supported by an NWO Vidi grant. DA acknowledges support from the Royal Society. NVG acknowledges funding from NOVA. JWH acknowledges funding from an NWO Vidi fellowship and from a European Research Council Starting Grant.

REFERENCES

- Altamirano D., Casella P., Patruno A., Wijnands R., Van Der Klis M., 2008, *ApJ*, 674, L45
- Archibald A. M. et al., 2009, *Science*, 324, 1411
- Armas Padilla M., Degenaar N., Patruno A., Russell D., Linares M., Maccarone T., Homan J., Wijnands R., 2011, *MNRAS*, 417, 659
- Bahramian A. et al., 2013, *ApJ*, 780, 127
- Bellini A. et al., 2013, *ApJ*, 765, 32
- Bozzo E. et al., 2011, *A&A*, 535, L1
- Bozzo E., Papitto A., Ferrigno C., Belloni T., 2014, *A&A*, 570, L2
- Bozzo E., Kuulkers E., Ferrigno C., 2015, *Astron. Telegram*, 7106, 1
- Chenevez J. et al., 2012, *Astron. Telegram*, 4050, 1
- Dalessandro E., Lanzoni B., Ferraro F., Rood R., Milone A., Piotto G., Valenti E., 2008, *ApJ*, 677, 1069
- Degenaar N., Wijnands R., 2012, *MNRAS*, 422, 581
- Degenaar N., Wijnands R., Cackett E., Homan J., in’t Zand J. J. M., Kuulkers E., Maccarone T., van der Klis M., 2012, *A&A*, 545, A49
- Degenaar N. et al., 2016, *MNRAS*, 461, 4049
- Del Santo M., Nucita A. A., Lodato G., Manni L., De Paolis F., Farihi J., De Cesare G., Segreto A., 2014, *MNRAS*, 444, 93
- Dickey J. M., Lockman F. J., 1990, *ARA&A*, 28, 215
- Ferrigno C., Bozzo E., Rodriguez J., Gibaud L., 2011, *Astron. Telegram*, 3566, 1
- Ferrigno C. et al., 2014, *A&A*, 567, A77
- Fridriksson J. K., Homan J., Remillard R. A., 2015, *ApJ*, 809, 52
- Galloway D. K., Cumming A., 2006, *ApJ*, 652, 559
- Güver T., Özel F., 2009, *MNRAS*, 400, 2050
- Harris W. E., 1996, *AJ*, 112, 1487
- Homan J. et al., 2010, *ApJ*, 719, 201
- Lewis F. et al., 2010, *A&A*, 517, A72
- Linares M. et al., 2014, *MNRAS*, 438, 251
- Ludlam R. et al., 2016, *ApJ*, 824, 37
- Ortolani S., Barbuy B., Bica E., 1994, *A&AS*, 108
- Ortolani S., Barbuy B., Bica E., Zoccali M., Renzini A., 2007, *A&A*, 470, 1043
- Papitto A. et al., 2013, *Nature*, 501, 517

- Parikh A. et al., 2017, *MNRAS*, 466, 4074
- Patruno A., Altamirano D., Hessels J. W., Casella P., Wijnands R., van der Klis M., 2009, *ApJ*, 690, 1856
- Patruno A., Maitra D., Curran P. A., D'Angelo C., Fridriksson J. K., Russell D. M., Middleton M., Wijnands R., 2016, *ApJ*, 817, 100
- Pintore F. et al., 2016, *MNRAS*, 457, 2988
- Plotkin R. M., Gallo E., Jonker P. G., 2013, *ApJ*, 773, 59
- Plotkin R. et al., 2016, *ApJ*, 834, 104
- Predehl P., Schmitt J. H., 1995, *A&A*, 293, 889
- Reynolds M. T., Reis R. C., Miller J. M., Cackett E. M., Degenaar N., 2014, *MNRAS*, 441, 3656
- Tetarenko A. et al., 2016, *MNRAS*, 460, 345
- Verner D., Ferland G., Korista K., Yakovlev D., 1996, *ApJ*, 465, 487
- Wachter K., Leach R., Kellogg E., 1979, *ApJ*, 230, 274
- Wijnands R., Heinke C. O., Pooley D., Edmonds P. D., Lewin W. H., Grindlay J. E., Jonker P. G., Miller J. M., 2005, *ApJ*, 618, 883
- Wijnands R., Degenaar N., Padilla M. A., Altamirano D., Cavecchi Y., Linares M., Bahramian A., Heinke C., 2015, *MNRAS*, 454, 1371
- Wilms J., Allen A., McCray R., 2000, *ApJ*, 542, 914

SUPPORTING INFORMATION

Supplementary data are available at *MNRAS* online.

Appendix.pdf

Figure A.1. The free N_{H} evolution with time for our six sources.

Figure B.1. The photon index Γ evolution with time for our six sources when the N_{H} is left free.

Figure C.1. The photon index versus luminosity (0.5–10 keV) for our six sources plotted for the N_{H} left free, the Galactic N_{H} , and the best-fit N_{H} value.

Please note: Oxford University Press is not responsible for the content or functionality of any supporting materials supplied by the authors. Any queries (other than missing material) should be directed to the corresponding author for the article.

This paper has been typeset from a \TeX/L\AA\TeX file prepared by the author.